

# Lattice-Reduction-Aided Preequalization over Algebraic Signal Constellations

Sebastian Stern and Robert F.H. Fischer

Institute of Communications Engineering, Ulm University, Ulm, Germany

Email: {sebastian.stern, robert.fischer}@uni-ulm.de

**Abstract**—Lattice-reduction-aided (LRA) equalization techniques have become very popular in multiple-input/multiple-output (MIMO) multiuser communication as they obtain the full diversity order of the MIMO channel. For joint transmitter-side LRA preequalization or precoding on the broadcast channel, the signal constellation is required to be periodically extendable, which is typically achieved by employing square QAM constellations. However, recent enhancements of the LRA philosophy—named integer-forcing equalization—additionally demand the data symbols to be representable as elements of a finite field over the grid the signal points are drawn from. This significantly constrains the choice of the constellation, especially when considering the complex baseband and complex-valued constellations. To overcome the lack of flexibility, in this paper, we present constellations with algebraic properties for use in LRA preequalization directly enabling the desired finite-field property. In particular, fields of Gaussian primes (integer lattice) and Eisenstein primes (hexagonal lattice) are studied and compared to conventional constellations. The respective transmitter- and receiver-side operations are detailed and the adaptation of the channel matrix factorization is proposed. Numerical simulations cover the performance of such schemes.

## I. INTRODUCTION

Multiple-input/multiple-output (MIMO) transmission has become one of the most significant approaches in nowadays wireless communication systems. Starting from point-to-point singleuser multi-antenna scenarios, research has rapidly been extended to multiuser multipoint-to-point transmission (multiple-access channel). In the sequel, by dualizing these results, a wide knowledge on the multiuser point-to-multipoint scenario (broadcast channel) could be obtained, e.g., [21], [22].

In order to shape the multiuser interference present on the broadcast channel, schemes well-known from singleuser transmission, e.g., Tomlinson-Harashima precoding (THP) [19], [9], have soon be adapted to the multiuser case [5], [3] since a simple linear preequalization (LPE) does not result in satisfactory performance. Unfortunately, even THP cannot take advantage of the MIMO channel's diversity: due to the inherent principle of *successive* interference cancellation, the diversity order remains one.

To overcome this problem, *lattice-reduction-aided* preequalization (LRA PE) and precoding have been proposed [25], [23], [24], [16], both achieving the full diversity order [18]. The main idea of LRA schemes is to perform the equalization in a suited basis, representing the distorted signal

grid. Thereby, integer linear combinations of the data are detected/decoded instead of the data itself. In a final step, these integer combinations are resolved. In THP and LRA preequalization/precoding, the choice of the signal constellation is restricted as it has to be periodically extendable [5]; usually square quadrature-amplitude modulation (QAM) constellations are employed.

Recently, so-called *integer-forcing (IF)* schemes have been introduced, which share the main idea of LRA equalization in detecting/decoding integer linear combinations. However, in IF the integer interference is resolved in the arithmetic of a finite field relaxing the unimodularity constraint on the integer matrix. This strategy was first introduced for receiver-side processing [14], [26], but has particularly been dualized to the broadcast channel [11], [10].

In IF, the crucial point is to link the signal constellation and the channel code to the arithmetic of a finite field. In [14], [26], this is done by restricting to real-valued modulation. For complex baseband channels, this is achieved by treating the quadrature components separately. In [11], specific square QAM constellations which form a field in the complex plane are applied. However, both approaches are very limited as only very specific constellation sizes are possible. An alternative strategy, already proposed for physical-layer network coding and relaying, is to draw the data symbols from algebraic structures over the complex plane, specifically, fields of so-called *Gaussian* or *Eisenstein primes* [17], [4], [20].

For transmitter-side LRA/IF equalization, these algebraic structures have not yet been considered in literature. Consequently, in this paper, we consider the application of algebraically-defined constellations in LRA PE. Both the complex-valued integer and hexagonal lattice are studied. The differences and advantages compared to state-of-the-art constellations are enlightened; in particular the possibility of periodically extending the constellation is of great importance in precoding. The performance of the different schemes is compared by means of numerical simulations.

The paper is structured as follows: In Sec. II, the system model for LRA PE on the MIMO broadcast channel is given. Sec. III briefly reviews signal constellations conventionally employed in LRA PE. In Sec. IV, algebraic signal constellations over Gaussian and Eisenstein integers are reviewed and their differences and advantages compared to the conventional ones are discussed. Numerical results are provided in Sec. V. The paper closes with a summary and conclusions in Sec. VI.

## II. SYSTEM MODEL

### A. MIMO Broadcast Channel Model

Throughout the paper, we assume a complex-valued (equivalent complex baseband) discrete-time MIMO broadcast channel; i.e., downlink transmission with joint transmitter-side processing and non-cooperating users is considered (cf. Fig. 1).

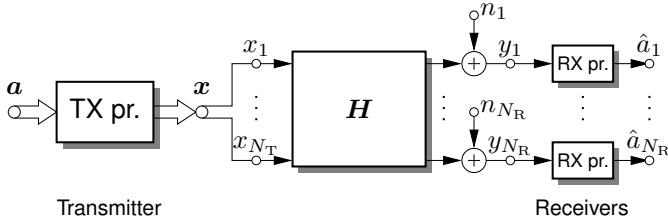


Fig. 1. MIMO broadcast channel model with joint transmitter-side processing (TX pr.) and non-collocated receivers (RX pr.).

In each time step, the data symbols  $a_l$  to be transmitted to receiver  $l = 1, \dots, N_R$ , in vector notation  $\mathbf{a} = [a_1, \dots, a_{N_R}]^T$ , are drawn from a predefined, zero-mean signal constellation  $\mathcal{A}$  with variance<sup>1</sup>  $\sigma_a^2 \stackrel{\text{def}}{=} \mathbb{E}\{|a|^2\}$  and cardinality  $M \stackrel{\text{def}}{=} |\mathcal{A}|$ ; hence, a rate  $R_m \leq \log_2(M)$  of (uncoded) modulation is achieved. Via transmitter-side processing, a vector of zero-mean transmit symbols  $\mathbf{x} = [x_1, \dots, x_{N_T}]^T$  to be radiated from the antennas is calculated. The sum transmit power is fixed to  $N_T \sigma_x^2 = N_R \sigma_a^2$  with  $\sigma_x^2 \stackrel{\text{def}}{=} \mathbb{E}\{|x|^2\}$ .

The MIMO broadcast channel is expressed by

$$\mathbf{y} = \mathbf{H}\mathbf{x} + \mathbf{n}, \quad (1)$$

where the MIMO channel matrix (flat-fading channel) reads

$$\mathbf{H} = [h_{l,k}]_{\substack{l=1,\dots,N_R \\ k=1,\dots,N_T}}. \quad (2)$$

We assume i.i.d. unit-variance zero-mean complex Gaussian distributed coefficients  $h_{l,k}$ , which are constant over a block of symbols (bursty transmission). On the channel, additive zero-mean white Gaussian noise  $\mathbf{n} = [n_1, \dots, n_{N_R}]^T$  with variance  $\sigma_n^2 \stackrel{\text{def}}{=} \mathbb{E}\{|n_l|^2\}$ ,  $l = 1, \dots, N_R$ , is present.

At the receivers, individual processing is performed; the vector of the resulting estimated data symbols is denoted as  $\hat{\mathbf{a}} = [\hat{a}_1, \dots, \hat{a}_{N_R}]^T$ .

The signal-to-noise ratio (SNR) is expressed as the transmitted energy per bit in relation to the average noise power spectral density, which reads

$$\frac{E_{b,\text{TX}}}{N_0} = \frac{\sigma_a^2}{\sigma_n^2 R_m}. \quad (3)$$

### B. Lattice-Reduction-Aided Preequalization

Lattice-reduction-aided preequalization or precoding [16], [24] is very well suited for handling the multiuser interference on the MIMO broadcast channel. To calculate the required

<sup>1</sup> $\mathbb{E}\{\cdot\}$  denotes expectation.

TX processing matrices, the augmented channel matrix is factorized according to [6]

$$\bar{\mathbf{H}} = [\mathbf{H} \quad \sqrt{\zeta}\mathbf{I}]_{N_R \times (N_R + N_T)} = \mathbf{Z}\bar{\mathbf{H}}_{\text{red}}, \quad (4)$$

where  $\zeta = \sigma_n^2/\sigma_x^2$  and  $\mathbf{I}$  is the identity matrix.  $\bar{\mathbf{H}}_{\text{red}}$  denotes the augmented reduced channel matrix and  $\mathbf{Z}$  is an unimodular integer matrix ( $|\det(\mathbf{Z})| = 1$ ). This factorization task can—in general—efficiently be performed via the LLL algorithm [13]. For the complex-valued situation at hand, the complex variant of the LLL algorithm [8] (denoted as “C-LLL”) is suited. Thus,  $\mathbf{Z}$  consists of complex integers (complex values with integers in both real- and imaginary part; represented by the Gaussian integers [12], [1], [2])

$$\mathbb{G} \stackrel{\text{def}}{=} \{z_I + jz_Q \mid z_I, z_Q \in \mathbb{Z}\}. \quad (5)$$

For LRA PE, the joint transmitter-side processing is performed as follows (see Fig. 2): Starting from the vector of data symbols  $\mathbf{a}$ , the LRA preequalization is performed via

$$\mathbf{a}_z = \mathbf{Z}^{-1}\mathbf{a} \quad (6)$$

where  $\mathbf{a}_z = [a_{z,1}, \dots, a_{z,N_R}]^T$ . Then, a component-wise modulo function  $\text{mod}_{\Lambda_p}(\cdot)$  w.r.t. some *precoding lattice*  $\Lambda_p$  is applied, resulting in a vector of precoded symbols  $\tilde{\mathbf{a}}_z = [\tilde{a}_{z,1}, \dots, \tilde{a}_{z,N_R}]^T$ . The modulo function generally reads

$$\text{mod}_{\Lambda}(z) \stackrel{\text{def}}{=} z - \mathcal{Q}_{\Lambda}(z), \quad z \in \mathbb{C}, \quad (7)$$

where

$$\mathcal{Q}_{\Lambda}(\cdot) \stackrel{\text{def}}{=} \underset{\lambda \in \Lambda}{\text{argmin}} |\lambda - z|^2 \quad (8)$$

denotes the quantization operation w.r.t. the given (complex) lattice  $\Lambda$ .

For LRA PE, just like for THP, the *signal point lattice*  $\Lambda_a$ , i.e., the grid the signal points are drawn from, and the precoding lattice  $\Lambda_p$  have to match in order to form a periodically extendable signal constellation [5]. This is usually achieved by choosing the signal constellation

$$\mathcal{A} \stackrel{\text{def}}{=} \mathcal{R}_V(\Lambda_p) \cap \Lambda_a, \quad (9)$$

where  $\mathcal{R}_V(\Lambda_p)$  denotes the *Voronoi region* of the precoding lattice; this region establishes the boundary region for the constellation by linking  $\Lambda_a$  and  $\Lambda_p$ . Further details will be explained in Sec. III.

When optimizing the preequalization according to the minimum mean-square error (MMSE) criterion, the residual linear preequalization can be performed via the  $N_T \times N_R$  upper part  $\mathbf{F}$  (preequalization matrix) of

$$\begin{bmatrix} \mathbf{F} \\ \mathbf{C} \end{bmatrix} \stackrel{\text{def}}{=} \bar{\mathbf{H}}_{\text{red}}^H \left( \bar{\mathbf{H}}_{\text{red}} \bar{\mathbf{H}}_{\text{red}}^H \right)^{-1} \quad (10)$$

and a channel-dependent scaling factor  $1/g$  to keep the average transmit power constant for each channel realization.

At the receiver side, each receiver scales its incoming signal with the factor  $g$ ; then a quantization with respect to  $\Lambda_a$  is applied, i.e.,

$$\tilde{a}_l = \mathcal{Q}_{\Lambda_a}(g \cdot y_l), \quad l = 1, \dots, N_R, \quad (11)$$

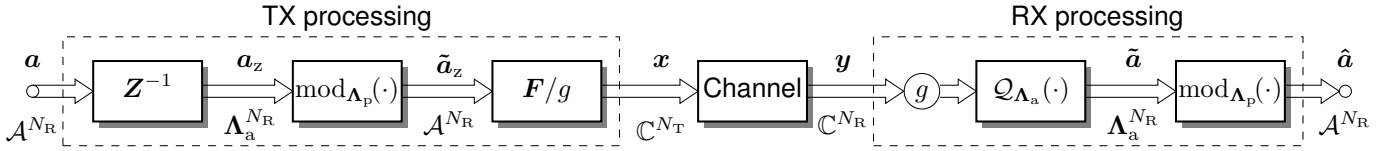


Fig. 2. LRA PE system model. Joint transmitter processing and non-cooperating receivers.

to obtain  $\tilde{\mathbf{a}} = [\tilde{a}_1, \dots, \tilde{a}_{N_R}]^T \in \Lambda_{\mathbf{a}}^{N_R}$ . Finally, estimated symbols  $\hat{\mathbf{a}} \in \mathcal{A}^{N_R}$  are obtained (from the modulo congruent ones) by applying the modulo function (7) w.r.t.  $\Lambda_{\mathbf{p}}$  to the quantized symbols  $\tilde{\mathbf{a}}$ .

### III. CONVENTIONAL LATTICE-REDUCTION-AIDED PREEQUALIZATION

In conventional LRA PE, the precoding lattice  $\Lambda_{\mathbf{p}}$  is typically chosen as a scaled version of the signal point lattice  $\Lambda_{\mathbf{a}}$ , mathematically  $\Lambda_{\mathbf{p}} = r\Lambda_{\mathbf{a}}$ , with  $r \in \mathbb{N}$ . The constellation is hence given as  $\mathcal{A} = \mathcal{R}_V(r\Lambda_{\mathbf{a}}) \cap \Lambda_{\mathbf{a}}$ . This case is now discussed in more detail.

#### A. Gaussian-Integer-Lattice Constellation

The common approach is to draw the data symbols from a subset of the ring of Gaussian integers, i.e.,  $\Lambda_{\mathbf{a}} = \mathbb{G}$  (isomorphic to lattice  $\mathbb{Z}^2$ , cf. [2]), and to choose the precoding lattice as a scaled version of  $\mathbb{G}$  in dependency of the desired cardinality, specifically  $\Lambda_{\mathbf{p}} = \sqrt{M}\mathbb{G}$ ,  $\sqrt{M} \in \mathbb{N}$ , for an  $M$ -ary signal constellation.

Consequently, square QAM constellations with  $\mathcal{A}_{\mathbb{G}} \stackrel{\text{def}}{=} \mathcal{A}_I + j\mathcal{A}_Q$  are obtained. If  $\sqrt{M}$  is an odd number, the constellation is immediately given as  $\mathcal{A}_I = \mathcal{A}_Q = \{0, \pm 1, \pm 2, \dots, (\sqrt{M} - 1)/2\}$ . For  $\sqrt{M}$  even, in order to be zero-mean,  $\mathcal{A}_I = \mathcal{A}_Q = \{\pm 1/2, \pm 3/2, \dots, (\sqrt{M} - 1)/2\}$ , is used; hence the shifted lattice  $\Lambda_{\mathbf{a}} + \mathbf{o} = \mathbb{G} + \mathbf{o}$  with offset  $\mathbf{o} = (1 + j)/2$  is present.<sup>2</sup> The variance of the constellation is given as  $\sigma_{\mathbf{a}}^2 = (M - 1)/6$ .

For  $z \in \mathbb{C}$ , the quantization to Gaussian integers reads<sup>3</sup>

$$Q_{\mathbb{G}}(z) = \lfloor \text{Re}\{z\} \rfloor + j \lfloor \text{Im}\{z\} \rfloor. \quad (12)$$

Since the precoding lattice is given as  $\Lambda_{\mathbf{p}} = \sqrt{M}\mathbb{G}$ , the modulo operation reads

$$\text{mod}_{\sqrt{M}\mathbb{G}}(z) = z - \sqrt{M} Q_{\mathbb{G}}\left(\frac{z}{\sqrt{M}}\right), \quad (13)$$

leading to a square boundary region  $\mathcal{R}_V(\sqrt{M}\mathbb{G})$ .

In Fig. 3, the 25-ary square QAM constellation is illustrated including the boundary region  $\mathcal{R}_V(5\mathbb{G})$ , as well as the constellation's periodic extensions. Noteworthy, each signal point has four nearest neighbor points (*kissing number*).

Moreover, the factorization of the channel matrix can be carried out via the C-LLL (entries of  $\mathbf{Z}$  are Gaussian integers).

<sup>2</sup>All operations explained in Sec. II have to be carried out w.r.t. the non-shifted lattice  $\Lambda_{\mathbf{a}}$ ; hence, the offset has to be compensated. Specifically,  $\mathbf{a}_z = \mathbf{Z}^{-1}(\mathbf{a} - \mathbf{o}) + \mathbf{o}$ , and the quantization of  $\tilde{\mathbf{y}} = \mathbf{g}\mathbf{y} - \mathbf{Z}\mathbf{o}$ , with  $\mathbf{o} = [o, \dots, o]^T$ , have to be performed.

<sup>3</sup> $\lfloor \cdot \rfloor$  denotes rounding to integers.

#### B. Eisenstein-Integer-Lattice Constellation

The ring of Eisenstein integers  $\mathbb{E}$  [2] represents the hexagonal grid in the complex plane (isomorphism from lattice  $\mathcal{A}_2$  to  $\mathbb{E}$ ) and is hence a potential alternative to the rectangular signal grid of the Gaussian integers.

A complex number is an Eisenstein integer if it can be written as

$$a + \omega b, \quad a, b \in \mathbb{Z}, \quad (14)$$

where  $\omega = (-1 + j\sqrt{3})/2 = e^{j2\pi/3}$ . Just like for Gaussian integers, a quantization to Eisenstein integers, denoted as  $Q_{\mathbb{E}}(z)$ ,  $z \in \mathbb{C}$ , is efficiently implementable [17].

As the hexagonal lattice (the Eisenstein integers) gives the densest packing possible in two dimensions [2], a *packing gain* can be achieved when choosing  $\Lambda_{\mathbf{a}} = \mathbb{E}$  instead of  $\Lambda_{\mathbf{a}} = \mathbb{G}$ . However, the number of neighboring signal points is increased to six. When additionally employing a scaled version of  $\mathbb{E}$  as precoding lattice  $\Lambda_{\mathbf{p}}$  (i.e., the boundary region  $\mathcal{R}_V(r\mathbb{E})$  is present), a *shaping gain* is possible, too [5]. As an example, in Fig. 4, a 25-ary zero-mean hexagonal constellation is illustrated for  $\Lambda_{\mathbf{p}} = 5\mathbb{E}$ .

Regrettably, the factorization with the complex LLL algorithm<sup>4</sup> is generally not possible for the Eisenstein integers: as it results in  $\mathbf{Z}$  consisting of Gaussian integers, we run out of the set  $\mathbb{E}$  when multiplying the vector of data symbols with  $\mathbf{Z}$  (e.g., an entry  $j$  leads to a phase rotation of  $\pi/2$  and hence a non-existent lattice point) and the lattice-reduction-aided preequalization becomes inoperative.<sup>5</sup>

### IV. LATTICE-REDUCTION-AIDED PREEQUALIZATION OVER ALGEBRAIC SIGNAL CONSTELLATIONS

In this section, the strategy of choosing the signal constellation  $\mathcal{A}$  for LRA preequalization according to algebraic structures is introduced.

In the following, the signal points are still drawn from  $\mathbb{G}$  or  $\mathbb{E}$ , i.e., we have the signal point lattice  $\Lambda_{\mathbf{a}} = \mathbb{G}$  or  $\Lambda_{\mathbf{a}} = \mathbb{E}$ . However, in contrast to the conventional approach mentioned in the previous section, the precoding lattice  $\Lambda_{\mathbf{p}}$  is now assumed to be a *complex* scaled version of  $\Lambda_{\mathbf{a}}$ , i.e.,  $\Lambda_{\mathbf{p}} = c\Lambda_{\mathbf{a}}$ , with  $c \in \mathbb{C}$ . This generalization raises the question how to choose  $c$  in order to obtain a periodically extendable constellation defined via (9).

<sup>4</sup>Or, alternatively: factorization using the conventional LLL algorithm with doubled dimension.

<sup>5</sup>A possible solution would be the restriction to *real-valued* entries of  $\mathbf{Z}$  (but the factorization has still to be applied to complex-valued channels). This can be achieved by restricting the quantization in the LLL algorithm to real-valued numbers; however, with a huge decrease in diversity order.

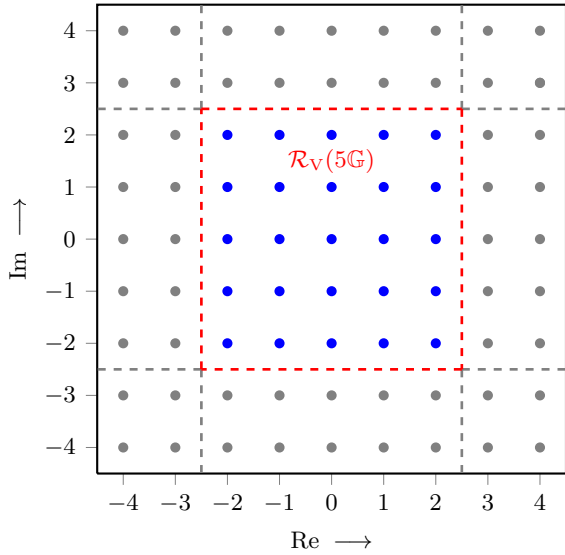


Fig. 3. Square QAM constellation  $\mathcal{A}_G$  for  $M = 25$  (blue;  $\Lambda_a = \mathbb{G}$ ,  $\Lambda_p = 5\mathbb{G}$ ). The boundary region is depicted (red dashed;  $\mathcal{R}_V(5\mathbb{G})$ ), as well as some signal points of the constellation's periodic extensions (gray).

The question can be answered with the help of algebraic structures—in particular finite fields over  $\mathbb{C}$ —, which inherently define a modulo congruence / modulo operation, hence a precoding lattice, and finally the signal constellation. For both  $\mathbb{G}$  and  $\mathbb{E}$ , such finite-field constellations are presented and their advantages in comparison to conventional LRA PE are discussed.

#### A. Gaussian Prime Constellations

1) *Preliminaries:* Consider a prime  $p > 2 \in \mathbb{N}$  of the form<sup>6</sup>  $\text{rem}_4(p) = 1$ , i.e.,  $p = 5, 13, 17, \dots$ . For this kind of real-valued primes, integers  $a, b \in \mathbb{Z}$ , and a Gaussian integer  $\Theta = a + jb \in \mathbb{G}$ , called a *Gaussian prime* [12], [1], can be found, which fulfill<sup>7</sup>

$$p = a^2 + b^2 = |a + jb|^2 = \Theta \Theta^*. \quad (15)$$

2) *LRA PE over Gaussian Prime Constellations:* For the case when  $\Lambda_a = \mathbb{G}$ , the basic idea is now to employ an (arbitrary) Gaussian prime as complex-valued scaling factor for the precoding lattice, i.e.,  $\Lambda_p = \Theta\mathbb{G}$ . The respective modulo function is consequently given by

$$\text{mod}_{\Theta\mathbb{G}}(z) = z - \Theta \mathcal{Q}_{\mathbb{G}}\left(\frac{z}{\Theta}\right), \quad (16)$$

and the signal constellation reads  $\mathcal{A}_{\Theta\mathbb{G}} \stackrel{\text{def}}{=} \mathcal{R}_V(\Theta\mathbb{G}) \cap \mathbb{G}$ . The boundary region  $\mathcal{R}_V(\Theta\mathbb{G})$  is hence still a square (cf. Fig. 3), but rotated by  $\arg(\Theta)$ .

The main advantage of the resulting Gaussian prime constellations over the conventional ones is that their data symbols (or the respective lattice points) inherently form a  $p$ -ary finite field over  $\mathbb{C}$ , denoted as  $\mathcal{G}_{\Theta}$  [12], [1]. The constellation's

<sup>6</sup> $\text{rem}_d(c) \stackrel{\text{def}}{=} c - d \lfloor c/d \rfloor$ , where  $c, d \in \mathbb{Z}$ .

<sup>7</sup> $\Theta^*$  denotes the complex conjugate of  $\Theta = a + jb$ , i.e.,  $\Theta^* = a - jb$ .

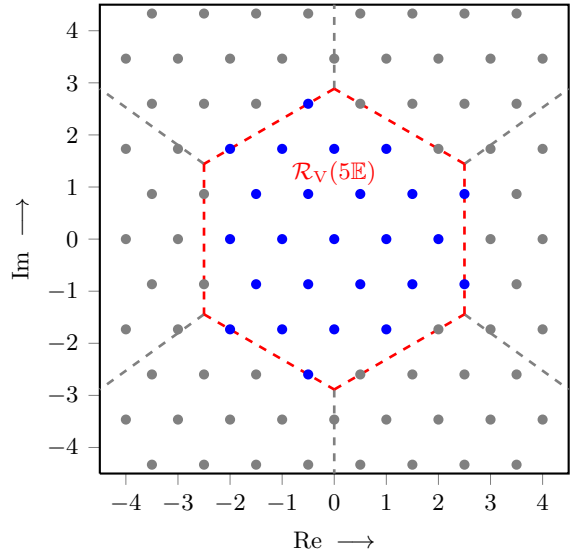


Fig. 4. 25-ary constellation  $\mathcal{A}_E$  over the hexagonal signal grid (blue;  $\Lambda_a = \mathbb{E}$ ,  $\Lambda_p = 5\mathbb{E}$ ). The boundary region is depicted (red dashed;  $\mathcal{R}_V(5\mathbb{E})$ ), as well as some signal points of the constellation's periodic extensions (gray).

cardinality is directly given as  $M = p = \Theta \Theta^*$  (cf. (15)). Since, in addition,

$$\text{mod}_{\Theta\mathbb{G}}(\gamma) \in \mathcal{G}_{\Theta}, \quad \forall \gamma \in \mathbb{G}, \quad (17)$$

defines a modulo function  $\mathbb{G} \rightarrow \mathcal{G}_{\Theta}$ , residue classes of  $\mathbb{G}$  modulo  $\Theta$ , the classes of modulo-congruent signal points, are immediate [12].  $\Lambda_a = \mathbb{G}$  and  $\Lambda_p = \Theta\mathbb{G}$  match in order to form a periodically extendable constellation, whose data symbols additionally represent a finite field over the complex plane. As an example, in Fig. 5, the 37-ary signal constellation based on  $\mathcal{G}_{\Theta}$ , where  $\Theta = 6 + j$ , is depicted.

Due to their point symmetry to  $z = 0$ , zero-mean Gaussian prime constellations are constructed. As in the conventional case, the common C-LLL can be applied, since  $\mathcal{Z}^{-1}$  consists of Gaussian integers and hence the LRA preequalized symbols  $\mathbf{a}_z$  (cf. (6)) also form a subset of  $\mathbb{G}$ . Noteworthy, due to (17), the precoded symbols  $\tilde{\mathbf{a}}_z$  are again elements of  $\mathcal{G}_{\Theta}$ . The same is valid after the receiver-side modulo operation, i.e.,  $\tilde{\mathbf{a}} \in \mathcal{G}_{\Theta}^{N_{\text{R}}}$ . Hence, an end-to-end finite-field channel is present.

3) *Isomorphism to  $\mathbb{F}_p$  or  $\mathbb{F}_{p^2}$ :* Noteworthy, an isomorphism between the finite field  $\mathbb{F}_p$ , where  $p = \Theta \Theta^*$  is a prime as defined above, and a corresponding finite field  $\mathcal{G}_{\Theta}$  over  $\mathbb{C}$  can be given [12], [1]. This fact can immediately be used to define a bijective mapping from  $\mathbb{F}_p$  to the signal constellation  $\mathcal{A}_{\Theta\mathbb{G}}$ , i.e., a labeling of the signal points via finite-field elements. Let  $\xi \in \mathbb{Z}_p = \{0, \dots, p-1\}$  be a real-valued integer representing the elements of  $\mathbb{F}_p$  ( $\mathbb{Z}_p \simeq \mathbb{F}_p$ ). Then, the corresponding signal point is simply given by  $a = \text{mod}_{\Theta\mathbb{G}}(\xi) \in \mathcal{A}_{\Theta\mathbb{G}}$ .

In addition, for primes  $p \in \mathbb{N}$  with  $\text{rem}_4(p) = 3$ , i.e.,  $p = 3, 7, 11, \dots$ , an isomorphism between the extension field  $\mathbb{F}_{p^2}$  and a field  $\mathcal{G}_{\Theta}$  with a Gaussian prime of the form  $\Theta = p$  or  $\Theta = jp$  is existent [12]. For these cases, the mapping to  $\mathcal{G}_{\Theta}$  is also defined by (16), but  $\xi \in \mathbb{Z}_p + j\mathbb{Z}_p$ . As a

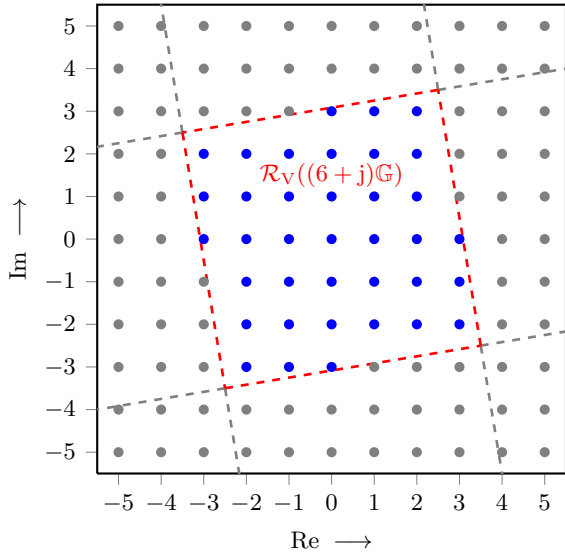


Fig. 5. Gaussian prime constellation  $\mathcal{A}_{\mathcal{G}_\Theta}$  for  $\Theta = 6 + j$  (blue;  $\Lambda_a = \mathbb{G}$ ,  $\Lambda_p = (6+j)\mathbb{G}$ ), i.e.,  $M = p = 37$ . Boundary region is depicted (red dashed;  $\mathcal{R}_V((6+j)\mathbb{G})$ ), as well as some signal points of the constellation's periodic extensions (gray).

consequence,  $M = p^2$ -ary Gaussian prime constellations  $\mathcal{A}_{\mathcal{G}_\Theta}$  with boundary region  $\mathcal{R}_V(p\mathbb{G}) = \mathcal{R}_V(j p\mathbb{G})$  are present. Since a rotation by  $\pi/2$  (multiplication by  $j$ ) does not influence the square boundary region, both cases are equivalent to the conventional square QAM one with cardinality  $\sqrt{M} = p$  per dimension (cf. (13) and Fig. 3). However, these special square QAM constellations represent finite fields in the complex plane. This property will be further discussed below.

### B. Eisenstein Prime Constellations

1) *Preliminaries:* Consider a prime  $p > 3 \in \mathbb{N}$  fulfilling  $\text{rem}_6(p) = 1$ , i.e.,  $p = 7, 13, 19, \dots$ . Then, an Eisenstein integer  $\Theta \in \mathbb{E}$  of the form  $\Theta = a + \omega b$ ,  $a, b \in \mathbb{Z}$ , called *Eisenstein prime* [17], can be found, for which holds

$$p = a^2 + b^2 - ab = |a + \omega b|^2 = \Theta \Theta^*. \quad (18)$$

2) *LRA PE over Eisenstein Prime Constellations:* In equivalence to the Gaussian prime constellations, Eisenstein prime constellations are obtained when choosing  $\Lambda_a = \mathbb{E}$  and  $\Lambda_p = \Theta\mathbb{E}$ , where  $\Theta$  is an Eisenstein prime as defined above. The modulo function now reads

$$\text{mod}_{\Theta\mathbb{E}}(z) = z - \Theta \mathcal{Q}_{\mathbb{E}}\left(\frac{z}{\Theta}\right), \quad (19)$$

and we obtain the signal constellation  $\mathcal{A}_{\mathcal{E}_\Theta} \stackrel{\text{def}}{=} \mathcal{R}_V(\Theta\mathbb{E}) \cap \mathbb{E}$ . Compared to the conventional case (cf. Fig. 4), the hexagonal boundary region  $\mathcal{R}_V(\Theta\mathbb{E})$  is maintained but it is again rotated in the complex plane by  $\arg(\Theta)$ .

In the same way as the Gaussian prime constellations, the signal points (data symbols) of the Eisenstein prime constellations form a  $p$ -ary finite field over  $\mathbb{C}$ , denoted as  $\mathcal{E}_\Theta$ , but naturally over the hexagonal signal grid [17], [20]. The

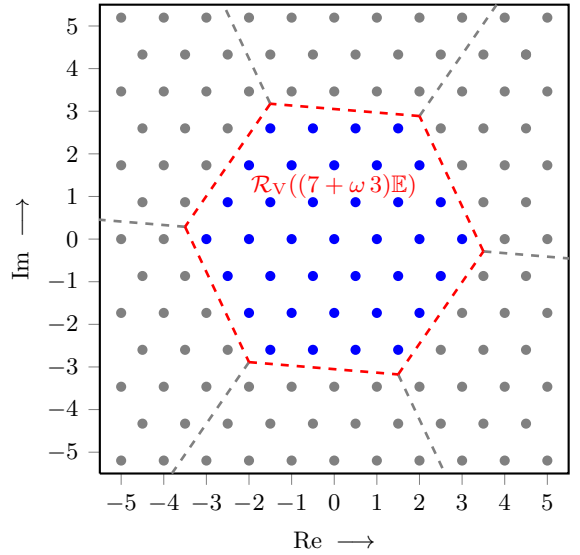


Fig. 6. Eisenstein prime constellation  $\mathcal{A}_{\mathcal{E}_\Theta}$  for  $\Theta = 7 + \omega 3$  (blue;  $\Lambda_a = \mathbb{E}$ ,  $\Lambda_p = (7 + \omega 3)\mathbb{E}$ ), i.e.,  $M = p = 37$ . Boundary region is depicted (red dashed;  $\mathcal{R}_V((7 + \omega 3)\mathbb{E})$ ), as well as some signal points of the constellation's periodic extensions (gray).

cardinality of  $\mathcal{E}_\Theta$  is hence given as  $M = p = \Theta \Theta^*$  (cf. (18)). Furthermore, as

$$\text{mod}_{\Theta\mathbb{E}}(\epsilon) \in \mathcal{E}_\Theta, \quad \forall \gamma \in \mathbb{E}, \quad (20)$$

we have a modulo function  $\mathbb{E} \rightarrow \mathcal{E}_\Theta$  and thus residue classes of  $\mathbb{E}$  modulo  $\Theta$ . Since  $\Lambda_a = \mathbb{E}$  and  $\Lambda_p = \Theta\mathbb{E}$  are matching, a periodically extendable constellation finite-field constellation is present. In Fig. 6, the 37-ary Eisenstein prime constellation, where  $\Theta = 7 + \omega 3$ , is exemplarily depicted.

3) *Factorization of the Channel Matrix:* For Eisenstein prime constellations, the common C-LLL algorithm does not result in a suitable matrix  $\mathbf{Z}$  (running out of lattice  $\mathbb{E}$ , cf. Sec. III). However, the finite-field property immediately offers a suited strategy: Let the entries of  $\mathbf{Z}$  (and hence  $\mathbf{Z}^{-1}$ ) now be drawn from  $\mathbb{E}$ ; we denote this matrix as  $\mathbf{Z}_{\mathbb{E}}$ . As a consequence, instead of quantizing to Gaussian integers ( $\mathcal{Q}_{\mathbb{G}}(\cdot)$ ) in the C-LLL algorithm [8, Line 1 in Alg. 2], the quantization operation is now performed with respect to the Eisenstein integers ( $\mathcal{Q}_{\mathbb{E}}(\cdot)$ ). The factorization task (4) hence reads

$$\bar{\mathbf{H}} = \mathbf{Z}_{\mathbb{E}} \bar{\mathbf{H}}_{\text{red}}. \quad (21)$$

We denote this variant of the LLL algorithm conducting a rounding to Eisenstein integers as ‘‘E-LLL’’.

When performing LRA PE, the preequalized symbols  $\mathbf{a}_z$  (cf. (6)) hence form a subset of  $\mathbb{E}$ . As a consequence, via  $\text{mod}_{\Theta\mathbb{E}}(\cdot)$ , elements of  $\mathcal{E}_\Theta$  are obtained (from the modulo congruent ones, cf. (20)), and thus  $\tilde{\mathbf{a}}_z \in \mathcal{E}_\Theta^{N_R}$ . At the receiver-side, after the modulo operation, the estimated symbols are again drawn from  $\mathcal{E}_\Theta$ . In summary, the end-to-end finite-field channel enables LRA/IF preequalization when operating over the hexagonal lattice. Noteworthy, all Eisenstein prime

constellations are zero-mean due to their point symmetry to  $z = 0$ .

4) *Isomorphism to  $\mathbb{F}_p$  or  $\mathbb{F}_{p^2}$* : The isomorphism between  $\mathbb{F}_p$  and  $\mathcal{E}_\Theta$  is similar to the one for  $\mathcal{G}_\Theta$  and gives the respective mapping from  $\mathbb{F}_p$  to the signal points; information, represented by  $\xi \in \mathbb{Z}_p \simeq \mathbb{F}_p$ , is mapped to the signal point via  $a = \text{mod}_{\Theta\mathbb{E}}(\xi) \in \mathcal{A}_{\mathcal{E}_\Theta}$

Moreover, an isomorphism between the extension field  $\mathbb{F}_{p^2}$  and a field of a related Eisenstein prime  $\Theta = p$  or  $\Theta = \omega p$  can be derived [17] when  $\text{rem}_3(p) = 2$ , i.e.,  $p = 2, 5, 11, \dots$ . The mapping to  $\mathcal{E}_\Theta$  is given by (19), but with  $\xi \in \mathbb{Z}_p + \omega \mathbb{Z}_p$ .

Regarding Eisenstein primes of the form  $\Theta = p$  or  $\Theta = \omega p$ ,  $p^2$ -ary signal constellations with  $\mathcal{R}_V(p\mathbb{E}) = \mathcal{R}_V(\omega p\mathbb{E})$  are obtained. Since a rotation by the Eisenstein unit  $\omega$  does not affect the hexagonal boundary region, we have equivalent constellations in both cases. In addition, the constellation illustrated in Fig. 4 turns out to be an Eisenstein prime one where  $\Theta = 5$  (or  $\Theta = \omega 5$ ). Hence, a finite-field constellation with  $M = p^2 = 25$  is given.

### C. Comparison to Conventional Case

In the following, we give an overview on the advantages of the described finite-field constellations in comparison to the conventional ones. Most important, the fact that they inherently specify a periodically extendable constellation with algebraic (finite-field) properties is highly desirable and a prerequisite for LRA/IF equalization/precoding. Furthermore, the benefit of a hexagonal signal grid / boundary region is discussed.

1) *Representation as Finite Field*: Recently, research activities have been focused on integer forcing schemes, e.g., [14], [11], [4], [26], which are very tightly related to the principle of LRA equalization. However, conventional (QAM) constellations are—in the main—not suited for these schemes as the idea is to resolve the interference via finite-field processing in combination with channel coding over these fields. For receiver-side equalization (multiple-access channel), the employment of fields of Gaussian and even Eisenstein integers [20] has already been proposed. However, for transmitter-side equalization/encoding, they are even more advantageous due to their implicitly defined modulo function.

Concerning conventional  $M$ -ary square QAM constellations, the naive approach to achieve a finite-field property is to separate the complex dimensions, i.e., splitting the constellation into  $\sqrt{M}$  one-dimensional fields  $\mathbb{Z}_{\sqrt{M}}$  with elements drawn from  $\mathbb{R}$ , isomorphic to  $\mathbb{F}_p$ , where  $p$  is a prime. However, as listed in Table I (column “ $(\mathbb{Z}_{\sqrt{M}})^2$ ”) for  $4 \leq M \leq 128$ , this strategy only results in five different possibilities ( $M = 4, 9, 25, 49, 121$ ); hence, the choice of the cardinality is very restricted.

In [11], for both transmitter- and receiver-side joint processing (multiple-access/broadcast channel), the employment of square QAM constellations representing fields over the complex plane is proposed (cf. isomorphism between  $\mathbb{F}_{p^2}$  and  $\mathcal{G}_\Theta$ ; purely real-valued  $\Theta$  w.r.t.  $\mathcal{G}_\Theta$  in Table I). This gives even less degrees of freedom ( $M = 9, 49, 121$ ).

TABLE I  
FINITE-FIELD CONSTELLATIONS FOR CARDINALITIES  $4 \leq M \leq 128$ .  
 $(\mathbb{Z}_{\sqrt{M}})^2$ ,  $\sqrt{M}$  A PRIME NUMBER, GAUSSIAN PRIME CONSTELLATIONS  
 $\mathcal{G}_\Theta$ ,  $\Theta$  A GAUSSIAN PRIME, AND EISENSTEIN PRIME CONSTELLATIONS  
 $\mathcal{E}_\Theta$ ,  $\Theta$  AN EISENSTEIN PRIME.

| $M$ | $(\mathbb{Z}_{\sqrt{M}})^2$ |              | $\mathcal{G}_\Theta$ |              | $\mathcal{E}_\Theta$ |              |
|-----|-----------------------------|--------------|----------------------|--------------|----------------------|--------------|
|     | $p$                         | $\sigma_a^2$ | $\Theta$             | $\sigma_a^2$ | $\Theta$             | $\sigma_a^2$ |
| 4   | 2                           | 0.5          |                      |              | 2                    | 0.75         |
| 5   |                             |              | $2 + j$              | 0.8          |                      |              |
| 7   |                             |              |                      |              | $3 + \omega$         | 0.8571       |
| 9   | 3                           | 1.3333       | 3                    | 1.3333       |                      |              |
| 13  |                             |              | $3 + j2$             | 2.1538       | $4 + \omega$         | 1.8462       |
| 17  |                             |              | $4 + j$              | 2.8235       |                      |              |
| 19  |                             |              |                      |              | $5 + \omega 2$       | 2.5263       |
| 25  | 5                           | 4            |                      |              | 5                    | 3.6          |
| 29  |                             |              | $5 + j2$             | 4.8276       |                      |              |
| 31  |                             |              |                      |              | $6 + \omega$         | 4.2581       |
| 37  |                             |              | $6 + j$              | 6.1622       | $7 + \omega 3$       | 5.0270       |
| 41  |                             |              | $5 + j4$             | 6.8293       |                      |              |
| 43  |                             |              |                      |              | $7 + \omega$         | 6            |
| 49  | 7                           | 8            | 7                    | 8            |                      |              |
| 53  |                             |              | $7 + j2$             | 8.8302       |                      |              |
| 61  |                             |              | $6 + j5$             | 10.1639      | $9 + \omega 4$       | 8.3607       |
| 67  |                             |              |                      |              | $8 + \omega 2$       | 9.3134       |
| 73  |                             |              | $8 + j3$             | 12.1644      | $9 + \omega$         | 10.1096      |
| 79  |                             |              |                      |              | $10 + \omega 3$      | 10.9367      |
| 89  |                             |              | $8 + j5$             | 14.8315      |                      |              |
| 97  |                             |              | $9 + j4$             | 16.1649      | $11 + \omega 3$      | 13.4845      |
| 101 |                             |              | $10 + j$             | 16.8317      |                      |              |
| 103 |                             |              |                      |              | $11 + \omega 2$      | 14.2718      |
| 109 |                             |              | $10 + j3$            | 18.1651      | $12 + \omega 5$      | 15.1927      |
| 113 |                             |              | $8 + j7$             | 18.8319      |                      |              |
| 121 | 11                          | 20           | 11                   | 20           | 11                   | 16.9091      |
| 127 |                             |              |                      |              | $13 + \omega 6$      | 17.5276      |

Skipping the square QAM property and going over to general fields of Gaussian primes (for  $\Lambda_a = \mathbb{G}$ ), the flexibility can tremendously be increased. As apparent from Table I, there are 14 additional cardinalities that can be chosen, all enabling finite-field calculations on complex symbols. While the above state-of-the-art approaches do not allow any cardinalities between  $M = 49$  and  $M = 121$ , employing the Gaussian prime constellations eight additional options are enabled.

2) *Advantages of Eisenstein Prime Constellations*: Two benefits are obtained when considering constellations  $\mathcal{A}_{\mathcal{E}_\Theta}$  based on the Eisenstein integers ( $\Lambda_a = \mathbb{E}$ ). On the one hand, the degree of freedom w.r.t. the cardinality is even more increased as constellations for 8 new values can be constructed (compared to  $\Lambda_a = \mathbb{G}$  for  $4 \leq M \leq 128$ , cf. Table I). Besides, for the cases  $M = 4$  and  $M = 25$ —which were only possible for separate component-wise processing—two-dimensional operations are possible here (isomorphism between  $\mathbb{F}_{p^2}$  and  $\mathcal{E}_\Theta$ ). On the other hand, positive impacts on the transmission performance can be expected: First, the packing and shaping gain of Eisenstein prime constellations in comparison to the Gaussian ones allow a decrease in transmit power (fixed desired error performance) or alternatively an increase in transmission performance (fixed transmit power). As an example, considering  $M = 61$ , where both fields of Gaussian and Eisenstein primes exist, a gain of about 0.85 dB concerning the variance of the respective constellations (cf.

Table I) is present. Moreover, the quantization to Eisenstein integers when applying the E-LLL algorithm results in a *factorization gain* compared to the Gaussian integers: due to the higher packing density, the average quantization error can be decreased. The consequence is a lower orthogonality defect and thus—finally—a lower noise enhancement.

## V. NUMERICAL RESULTS

In the following, the theoretical considerations and derivations from the previous sections are covered by means of numerical simulations. For fair comparison, all simulations were performed w.r.t. the basic LRA PE system model for the  $N_R \times N_T$  i.i.d. flat-fading MIMO broadcast channel as described in Sec. II. Factorization of the augmented channel matrix is done via C-LLL (or E-LLL, respectively) as efficient factorization algorithms for the IF strategy are not yet available (cf. [15]). The linear preequalization part is adjusted according to the MMSE criterion. For comparison, in each case, the results for conventional linear preequalization according to the MMSE criterion are given.<sup>8</sup> The presented results are averaged over the users and a sufficiently large number of channel realizations.

### A. Transmission using Finite-Field Constellations

First, we assess Gaussian or Eisenstein prime constellations and compare them to conventional square QAM constellations of similar cardinalities that may be represented as (one-dimensional or complex-valued) finite fields. In the figures, the symbol error rate (SER) in dependency of  $E_{b,TX}/N_0$  is given. Noteworthy, even when considering non-binary uncoded transmission (i.e.,  $R_m \notin \mathbb{N}$ ), the energy per bit as opposed to the energy per symbol is more appropriated since the amount of transmitted information per modulation step is taken into account.

1) *Scenario 1*: In Fig. 7, a 9-ary square QAM constellation ( $\mathcal{A}_G$ ), representable as Gaussian prime constellation  $\mathcal{A}_{G_\Theta}$ , where  $\Theta = 3$ , serves as basis for the comparison. In addition, the performance of Gaussian prime constellations with cardinalities  $M = 5$  and  $M = 13$  is given. These constellations have the same signal point lattice  $\Lambda_a$  and a (possibly rotated) square Voronoi region of  $\Lambda_p$ . First, we restrict to the case  $N_T = N_R = 4$  (top). Obviously, decreasing the cardinality from  $M = 9$  ( $R_m = 3.17$ ) to  $M = 5$  ( $R_m = 2.32$ ) leads to a gain of approximately 1.25 dB in  $E_{b,TX}/N_0$  in the low-SER regime, whereas an increase from  $M = 9$  to  $M = 13$  ( $R_m = 3.70$ ) induces a loss of about 1.75 dB, while the constellations' basic properties stay the same. We hence obtain more flexibility in the trade-off between spectral efficiency (high  $R_m$ ) and power efficiency (low transmit power) when including (general) Gaussian prime constellations.

With regard to the hexagonal lattice constellations, the impact of the packing, shaping, and factorization gain becomes apparent: In comparison to the lattice  $\mathbb{G}$ , for  $M = 13$ , a gain of

<sup>8</sup>Conventional linear preequalization is equivalent to LRA PE with  $\mathbf{Z} = \mathbf{I}$  and switching off all modulo operations.

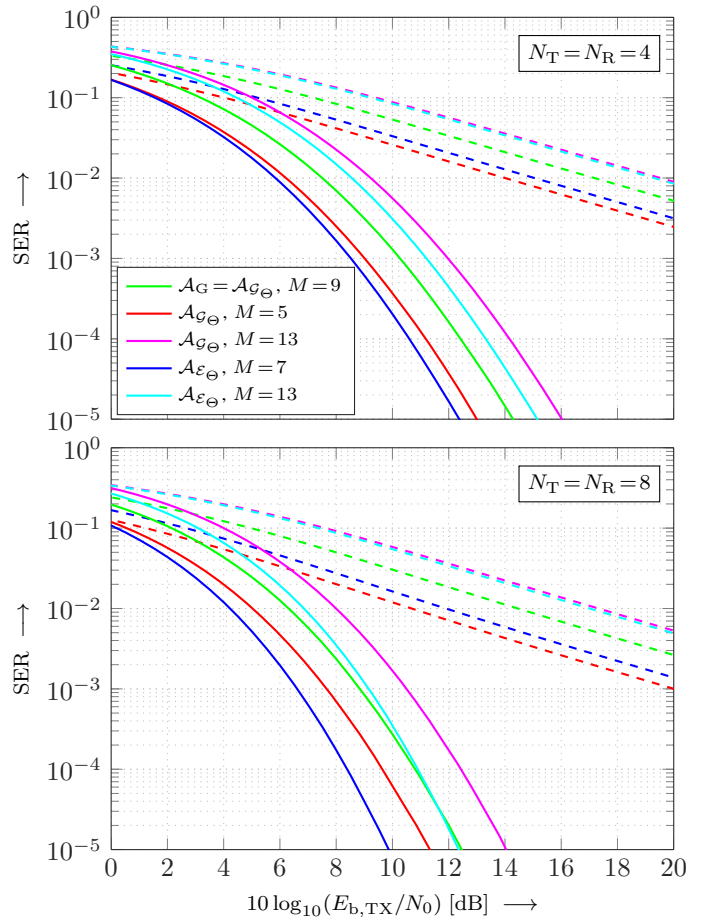


Fig. 7. SER over  $E_{b,TX}/N_0$  for uncoded LRA PE employing finite-field constellations according to Scenario 1 (solid). Parameter:  $M$ ; variation of signal point lattice  $\Lambda_a$ . For comparison, the results for conventional LPE are given (dashed). Top:  $N_T = N_R = 4$ . Bottom:  $N_T = N_R = 8$ .

about 1 dB is present in the high-SNR regime. Moreover, the 7-ary Eisenstein prime constellation even exhibits a lower SER than the 5-ary Gaussian one. Thus, if possible, the Eisenstein lattice should be preferred.

For the situation at hand, all curves converge to diversity order four ( $E_{b,TX}/N_0 \rightarrow \infty$ ). Due to equalization according to the MMSE criterion, the decline may even be larger in the mid-to-high-SNR regime, but the curves finally flatten out to this slope. For the conventional LPE case, the rapid convergence to diversity order one is clearly visible. Here, the Eisenstein constellations show hardly any advantage, as the number of six nearest neighbors more degrades the overall performance since the slope of the curve is small.

Fig. 7 (bottom) additionally visualizes the results for the abovementioned constellations if  $N_T = N_R = 8$ . Due to the higher diversity and larger receive power (for fixed transmit power), the SER is typically lower for a fixed SNR. All LRA PE curves finally converge to diversity order eight, whereas the order for conventional LPE cannot be increased. Again, the more flexible trade-off between spectral and power efficiency enabled by using Gaussian prime constellations is visible;

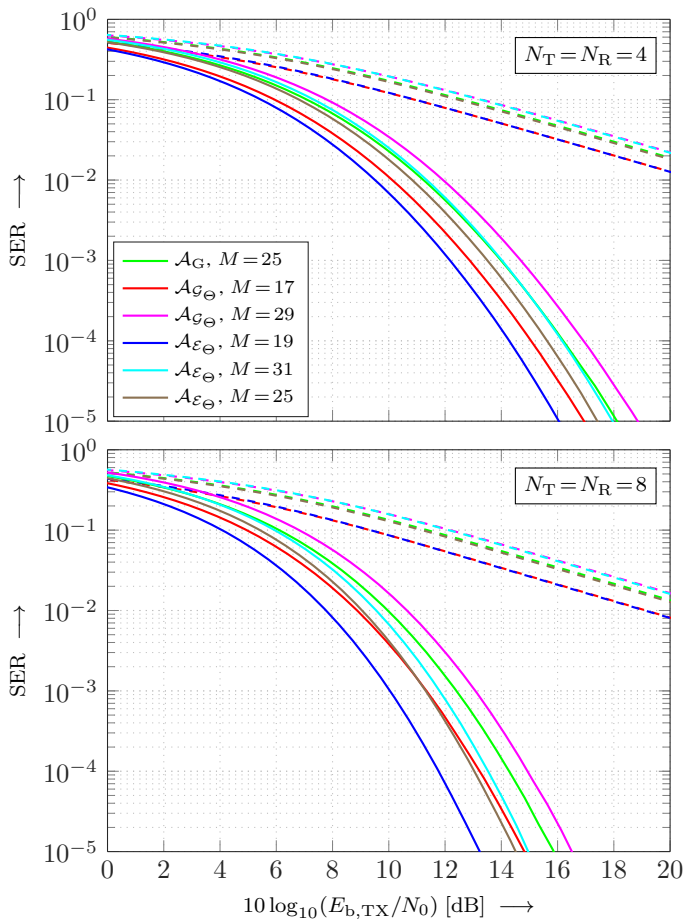


Fig. 8. SER over  $E_{b,TX}/N_0$  for uncoded LRA PE employing finite-field constellations according to Scenario 2 (solid). Parameter:  $M$ ; variation of signal point lattice  $\Lambda_a$ . For comparison, the results for conventional LPE are given (dashed). Top:  $N_T = N_R = 4$ . Bottom:  $N_T = N_R = 8$ .

the gap w.r.t.  $E_{b,TX}/N_0$  even becomes larger. Besides, the Eisenstein prime constellations are actually more advantageous for high diversities; the 13-ary Eisenstein one almost performs the same as the 9-ary square QAM one.

2) *Scenario 2*: In addition, we consider a scenario where a 25-ary square QAM constellation is taken as basis.<sup>9</sup> The respective simulation results are depicted in Fig. 8. Restricting  $\Lambda_a$  to  $\mathbb{G}$ , again we can utilize the improved degrees of freedom concerning the cardinality and hence obtain a more flexible and fine-granular trade-off between power and spectral efficiency.

The superiority of the Eisenstein constellations is again present, e.g., for the case  $N_T = N_R = 4$ , the 31-ary Eisenstein constellation shows the same performance as the 25-ary Gaussian one. When assuming  $N_T = N_R = 8$ , even though the rate is increased from  $R_m = 4.64$  to  $R_m = 4.95$ , a gain of about 0.5 dB in  $E_{b,TX}/N_0$  (high-SNR regime) is achieved for

<sup>9</sup>Noteworthy, for the lattice  $\mathbb{G}$ , this constellation can only be represented via one-dimensional finite fields  $\mathbb{Z}_{\sqrt{M}}$ ; a complex-valued finite-field representation as in the previous scenario is not possible.

TABLE II  
BINARY TRANSMISSION: SIMULATION PARAMETERS AND PROPERTIES

| Constellation                            | $\beta$ | $\mu$ | $R_m$ | $2^\beta/M^\mu$ |
|--|---------|-------|-------|-----------------|
| $\mathcal{A}_{\mathbb{G}}, M = 64$       | 6       | 1     | 6     | 1               |
| $\mathcal{A}_{\mathbb{G}\Theta}, M = 61$ | 427     | 72    | 5.93  | 0.9910          |
| $\mathcal{A}_{\mathbb{E}\Theta}, M = 61$ | 427     | 72    | 5.93  | 0.9910          |
| $\mathcal{A}_{\mathbb{E}\Theta}, M = 67$ | 6       | 1     | 6     | 0.9552          |

the considered Eisenstein constellation.<sup>10</sup> In addition, for the scenario at hand, the comparison of a 25-ary Gaussian to a 25-ary Eisenstein constellation is possible (cf. isomorphism between  $\mathbb{F}_{p^2}$  and  $\mathbb{E}_\Theta$ ). Considering  $N_T = N_R = 8$ , the Eisenstein one gains approximately 1 dB.

As above, all curves for LRA PE converge to diversity order four ( $N_T = N_R = 4$ ) or eight ( $N_T = N_R = 8$ ), respectively; conventional LPE inherently has diversity order one.

### B. Binary Transmission

Finally, we consider the case of binary end-to-end transmission, i.e., include the mapping from binary data to signal points and vice versa into the end-to-end model. Here, square QAM constellations with  $R_m = \log_2(M) \in \mathbb{N}$  are the most natural choice as a direct mapping from  $\beta = \log_2(M)$  bits to one data symbol can be performed.

Unfortunately, a straightforward mapping from bits to data symbols is not possible when employing Gaussian or Eisenstein prime constellations, as  $R_m = \log_2(p) \notin \mathbb{N}$  (or  $R_m = \log_2(p^2) \notin \mathbb{N}$ , respectively).<sup>11</sup> The following approaches solve this problem:

i) Blocks of  $\beta$  bits, i.e.,  $\mathbf{b} = [b_1, \dots, b_\beta]$ , are mapped to blocks of  $\mu$  data symbols, i.e.,  $\mathbf{m} = [m_1, \dots, m_\mu]$ , by means of *modulus conversion* [7], [5].  $M^\mu \geq 2^\beta$  has to hold; the surplus signal point vectors are neglected leading to a degradation. The modulation rate is given by  $R_m = \beta/\mu$ . At the receiver side, the inverse of modulus conversion is performed to recover the bits from the estimated symbols.

ii)  $2^\beta$ -ary transmission with an  $M$ -ary constellation ( $M > 2^\beta$ ), i.e.,  $M - 2^\beta$  potential data symbols are ignored. This strategy can be interpreted as a modulus conversion with parameter  $\mu = 1$ .

Starting from a 64-ary square QAM constellation, both the 61-ary Gaussian and Eisenstein prime constellations are suited for a comparison, as well as the 67-ary Eisenstein one. For the 61-ary constellations, we apply modulus conversion in order to map bits to symbols; the parameters are given in Table II.<sup>12</sup> In contrast, for  $\mathcal{A}_{\mathbb{E}\Theta}$  with  $M = 67$ , three potential signal points are dropped to obtain a 64-ary constellation. In this case—to be zero-mean—it is convenient to exclude two opposing

<sup>10</sup>Even though the 25-ary Gaussian prime constellation has a lower variance than the 31-ary Eisenstein one (cf. Table I), the Eisenstein constellation performs better due to the factorization gain.

<sup>11</sup>The case  $M = p^2 = 4$  is an exception, cf. Table I.

<sup>12</sup>Since not all  $M^\mu$ , but only  $2^\beta$  signal point vectors are used, the signal points are not precisely drawn with equal probability. Hence, a mean will be present. For large block lengths in the modulus conversion, however, this mean value is very low in comparison to the constellation's variance. Nevertheless, this fact is incorporated in the simulation results.



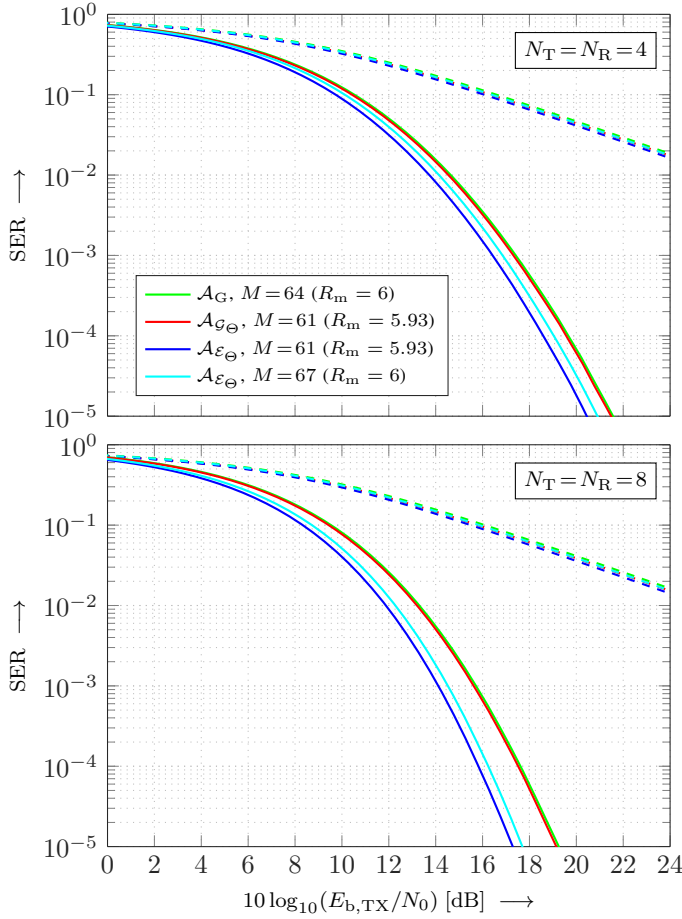


Fig. 9. SER over  $E_{b,TX}/N_0$  for LRA PE assuming uncoded binary end-to-end transmission according to Table II (solid). Parameter:  $M$ ; variation of signal point lattice  $\Lambda_a$ . For comparison, the results for conventional LPE are given (dashed). Top:  $N_T = N_R = 4$ . Bottom:  $N_T = N_R = 8$ .

signal points with the largest magnitude (e.g.,  $a = 2 + \omega 5$  and  $a = -2 - \omega 5$ ), and also the signal point located at the origin ( $a = 0$ ).

Fig. 9 illustrates the symbol error rate for binary transmission in dependency of  $E_{b,TX}/N_0$  subject to Table II for both  $N_T = N_R = 4$  and  $N_T = N_R = 8$ . The conclusions that can be drawn from these SER plots are similar to the ones for the previous finite-field scenarios: transmission performance increases with the diversity order, and the Eisenstein prime constellations allow a decrease in  $E_{b,TX}/N_0$  due to their packing, shaping, and factorization gain. For  $N_T = N_R = 8$  we have a gain of about 1.75 dB for the 67-ary-based 64-ary Eisenstein constellation compared to the 64-ary square QAM one.<sup>13</sup> Instead, employing the 61-ary Eisenstein one results in a minor additional gain. Similarly, both Gaussian-prime-based constellations nearly perform the same. For conventional LPE, the transmission performance is nearly almost constant over all considered constellations; again only diversity order one is

<sup>13</sup>Noteworthy, the 64-ary Eisenstein-based constellation has the variance  $\sigma_a^2 = 9.1562$ .

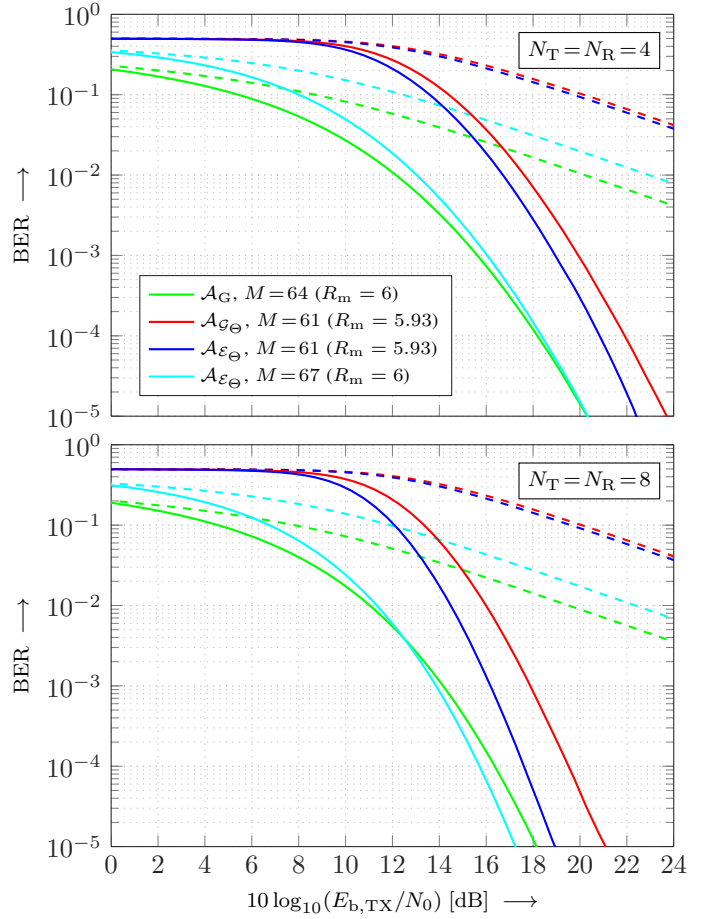


Fig. 10. BER over  $E_{b,TX}/N_0$  for LRA PE assuming uncoded binary end-to-end transmission according to Table II (solid). Parameter:  $M$ ; variation of signal point lattice  $\Lambda_a$ . For comparison, the results for conventional LPE are given (dashed). Top:  $N_T = N_R = 4$ . Bottom:  $N_T = N_R = 8$ .

possible.

When assuming binary (uncoded) transmission, the bit-error rate (BER) is of great importance. In Fig. 10, it is plotted over  $E_{b,TX}/N_0$ , again for  $N_T = N_R = 4$  and  $N_T = N_R = 8$ , respectively. Obviously, binary transmission based on modulus conversion results in a rather poor BER performance in the low-to-mid-SNR regime. This can easily be explained by error propagation when carrying out the inverse modulus conversion in the receivers: one single symbol error over the block of  $\mu$  symbols affects the whole block of equivalent  $\beta$  bits. In contrast, if a direct mapping to one symbol is used, only  $\log_2(M)$  bits are affected. For the 64-ary square QAM constellation, a Gray labeling can be employed—then each symbol error causes only a single bit error (in the mid-to-high-SNR regime). Regrettably, for the Gaussian and Eisenstein prime constellations, a Gray labeling cannot be given in general (and has no direct meaning if modulus conversion is applied). To summarize, for uncoded transmission, a mapping via modulus conversion is rather critical. Nevertheless, in the low-BER range ( $BER \approx 10^{-5}$ ) for the high-diversity case, the 61-ary Eisenstein prime constellation nearly achieves the performance

of the 64-ary square QAM one.

Concerning the 64-ary (67-ary-based) Eisenstein constellation, the situation is different: Since the abovementioned error propagation is not relevant in this case, in the low-to-mid-SNR range (as well as for non-LRA LPE) only the lack of a Gray labeling becomes apparent. In the high-SNR regime, the packing, shaping, and factorization gain are the more dominating quantities and the Eisenstein constellation shows at least the same performance as the square QAM one ( $N_R = N_T = 4$ ). For the high-diversity case,  $N_R = N_T = 8$ , a gain of approximately 1 dB is possible. Thus, the employment of Eisenstein prime constellations can even be advantageous for uncoded binary end-to-end transmission, if a suitable mapping from bits to field elements can be found.

## VI. SUMMARY AND CONCLUSIONS

In this paper, the approach of choosing algebraic signal constellations for lattice-reduction-aided preequalization on the MIMO broadcast channel has been presented and assessed. First, conventional complex-valued constellations and their properties have briefly been reviewed. Basic conditions and properties w.r.t. fields of Gaussian and Eisenstein primes have been discussed, as well as the possibility to apply them as algebraic signal constellations for LRA PE. Their similarities and differences to the conventional ones have been worked out, especially concerning the finite-field property, the flexibility of choosing the cardinality, and the shaping, packing, and factorization gain of (hexagonal) Eisenstein constellations. The theoretically-based derivations have been complemented by numerical simulations revealing the usefulness of these algebraic signal constellations in precoding schemes.

The finite-field property of these constellations is indispensable for integer-forcing schemes. In this paper, due to lack of space, only uncoded transmission has been presented. However, the exposed constellation design can immediately be combined with coding techniques. As the fields of Gaussian and Eisenstein primes are isomorphic to  $\mathbb{F}_p$ , a perfect match is obtained when applying coded modulation via non-binary  $p$ -ary codes, e.g., low-density-parity-check codes over  $\mathbb{F}_p$  [11], [20]. Using algebraic signal constellations, suited non-binary codes, and LRA/IF equalization/preequalization schemes, a perfect cooperation of the three parts with flexible design is enabled.

## REFERENCES

- [1] M. Bossert. *Channel Coding for Telecommunications*. John Wiley & Sons Ltd, 1999.
- [2] J. Conway, N.J.A. Sloane. *Sphere Packings, Lattices and Groups*. Third Edition, Springer, 1999.
- [3] U. Erez, S. Shamai, R. Zamir. Capacity and Lattice Strategies for Canceling Known Interference. *IEEE Transactions on Information Theory*, pp. 3820–3833, Nov. 2005.
- [4] C. Feng, D. Silva, F.R. Kschischang. An Algebraic Approach to Physical-Layer Network Coding. *IEEE Transactions on Information Theory*, pp. 7576–7596, Nov. 2013.
- [5] R.F.H. Fischer. *Precoding and Signal Shaping for Digital Transmission*. Wiley-IEEE Press, 2002.
- [6] R.F.H. Fischer. Complexity-Performance Trade-Off of Algorithms for Combined Lattice Reduction and QR Decomposition. *International Journal of Electronics and Communications (AEÜ)*, pp. 871–879, Nov. 2012.
- [7] G.D. Forney, G. Ungerböck. Modulation and Coding for Linear Gaussian Channels. *IEEE Transactions on Information Theory*, pp. 2384–2415, Oct. 1998.
- [8] Y.H. Gan, C. Ling, W.H. Mow. Complex Lattice Reduction Algorithm for Low-Complexity Full-Diversity MIMO Detection. *IEEE Transactions on Signal Processing*, pp. 2701–2710, July 2009.
- [9] H. Harashima, H. Miyakawa. Matched-Transmission Technique for Channels with Intersymbol Interference. *IEEE Transactions on Communications*, pp. 774–780, Aug. 1972.
- [10] W. He, B. Nazer, S. Shamai. Uplink-Downlink Duality for Integer-Forcing. In *IEEE International Symposium on Information Theory*, pp. 2544–2548, June/July 2014.
- [11] S.N. Hong, G. Caire. Compute-and-Forward Strategies for Cooperative Distributed Antenna Systems. *IEEE Transactions on Information Theory*, pp. 5227–5243, May 2013.
- [12] K. Huber. Codes over Gaussian Integers. *IEEE Transactions on Information Theory*, pp. 207–216, Jan. 1994.
- [13] A.K. Lenstra, H.W. Lenstra, L. Lovasz. Factoring Polynomials with Rational Coefficients. *Mathematische Annalen*, pp. 515–534, 1982.
- [14] B. Nazer, M. Gastpar. Compute-and-Forward: Harnessing Interference Through Structured Codes. *IEEE Transactions on Information Theory*, pp. 6463–6486, Oct. 2011.
- [15] A. Sakzad, J. Harshan, E. Viterbo. On Complex LLL Algorithm for Integer Forcing Linear Receivers. In *2013 Australian Communications Theory Workshop*, pp. 13–17, Jan./Feb. 2013.
- [16] C. Stierstorfer, R.F.H. Fischer. Lattice-Reduction-Aided Tomlinson-Harashima Precoding for Point-to-Multipoint Transmission. *International Journal of Electronics and Communications (AEÜ)*, pp. 328–330, 2006.
- [17] Q.T. Sun, J. Yuan, T. Huang, K.W. Shum. Lattice Network Codes Based on Eisenstein Integers. *IEEE Transactions on Communications*, pp. 2713–2725, July 2013.
- [18] M. Taherzadeh, A. Mobasher, A.K. Khandani. LLL Reduction Achieves the Receive Diversity in MIMO Decoding. *IEEE Transactions on Information Theory*, pp. 4801–4805, Dec. 2007.
- [19] M. Tomlinson. New Automatic Equalizer Employing Modulo Arithmetic. *Electronic Letters*, pp. 138–139, Mar. 1971.
- [20] N.E. Tunali, Y.C. Huang, J.J. Boutros, K.R. Narayanan. *Lattices over Eisenstein Integers for Compute-and-Forward*. Available online: <http://arxiv.org/abs/1404.1312>, v2, Oct. 2014.
- [21] P. Viswanath, D.N.C. Tse. Sum Capacity of the Vector Gaussian Broadcast Channel and Uplink-Downlink Duality. *IEEE Transactions on Information Theory*, pp. 1912–1921, Aug. 2003.
- [22] S. Vishwanath, N. Jindal, A. Goldsmith. Duality, Achievable Rates, and Sum-Rate Capacity of Gaussian MIMO Broadcast Channels. *IEEE Transactions on Information Theory*, pp. 2658–2668, Oct. 2003.
- [23] C. Windpassinger, R.F.H. Fischer. Low-Complexity Near-Maximum-Likelihood Detection and Precoding for MIMO Systems Using Lattice Reduction. *Proc. IEEE Information Theory Workshop*, pp. 345–348, Mar. 2003.
- [24] C. Windpassinger, R.F.H. Fischer, J.B. Huber. Lattice-Reduction-Aided Broadcast Precoding. *IEEE Transactions on Communications*, pp. 2057–2060, Dec. 2004.
- [25] H. Yao, G.W. Wornell. Lattice-Reduction-Aided Detectors for MIMO Communication Systems. *Proc. IEEE Global Telecommunications Conference*, Taipei, Taiwan, Nov. 2002.
- [26] J. Zhan, B. Nazer, U. Erez, M. Gastpar. Integer-Forcing Linear Receivers. *IEEE Transactions on Information Theory*, pp. 7661–7685, Oct. 2014.